Available online at www.sciencedirect.com
ScienceDirect
Trans. Nonferrous Met. Soc. China 34(2024) 547−559
Transactions of Nonferrous Metals Society of China
www.tnmsc.cn

Characterization, wear behavior and biocompatibility of HA/Ti composite and functionally graded coatings deposited on Ti−6Al−4V substrate by mechanical coating technique

Mahmood JALALI BIDAKHAVIDI[1], Hamid OMIDVAR[1], Ali ZAMANIAN[2], Jamshid AGHAZADEH MOHANDESI[1], Hamid JALALI[3]

1. Department of Materials and Metallurgical Engineering, Amirkabir University of Technology (Tehran Polytechnic), Hafez Ave, P.O. Box 15875-4413, Tehran, Iran;
2. Department of Nanotechnology and Advanced Materials, Materials and Energy Research Center, Karaj, Iran;
3. School of Dentistry, Tehran University of Medical Sciences, Tehran, Iran

Received 6 August 2022; accepted 28 February 2023

Abstract: Characterization, wear behavior, and biocompatibility of hydroxyapatite (HA)/Ti composite coating and functionally graded coatings (FGCs) deposited on a Ti−6Al−4V substrate by a mechanical coating technique were compared. The composite coating was produced using the initial powder mixture of 50 wt.% Ti + 50 wt.% HA, while the FGC was deposited by two separate layers containing 75 wt.% Ti + 25 wt.% HA and 25 wt.% Ti + 75 wt.% HA, respectively. The XRD results exhibited that no phase changed during the deposition process. Moreover, due to the presence of Ti particles in the primary powder mixtures, a continuous interface with a superior bond was formed between the coating and the substrate, especially in the samples coated by the FGCs. The wear test results of the non-graded composite coating showed a coefficient of friction (COF) of about 0.37 with an abrupt change at the interface, while the COF of the FGCs increased from 0.32 to 0.5 with a gentle change at the interface. The SEM images of the worn surfaces indicated the dominance of the abrasive wear mechanism. The biocompatibility evaluations revealed better cell attachment and proliferation of the FGC-coated samples.

Key words: mechanical coating technique; hydroxyapatite; Ti−6Al−4V substrate; functionally graded coating; coefficient of friction

1 Introduction

Titanium alloy is one of the best metallic materials used in biomedical applications, of which Ti−6Al−4V, as one of the most widely-used hard tissue alternative materials, is employed in different areas, such as dental implants, knee and hip prostheses, and artificial joints and bones, due to its excellent properties, such as high yield strength, proper fracture toughness, low density, and corrosion resistance [1,2]. However, when used as an implant, there is a possibility of chemical dissolution or wear in the body (even in small amounts). Moreover, after implantation, the implant is surrounded by a fibrous tissue because of limited bone growth and weak surface bonding to the neighboring tissue. A proposed solution to minimize these disadvantages is to deposit a suitable biocompatible coating on the surface of the implant. As a result, a metallic substrate with excellent mechanical properties and better bone growth rate is achieved and implant-body undesirable interactions are eliminated [3−6].

For this purpose, hydroxyapatite (HA) is one of the most suitable bioceramic materials that have

Corresponding author: Hamid OMIDVAR, E-mail: omidvar@aut.ac.ir
DOI: 10.1016/S1003-6326(23)66416-7

been used for deposition on the metallic implants. Its structure and chemical composition are similar to those of natural bone mineral and it is sufficiently biocompatible and bioactive, thereby the new bone can be immediately formed on it [7,8]. However, due to the inherent differences in mechanical and physical properties of ceramics and metals, deposition of HA on metal substrates is problematic. Efforts have been made to surmount the problems by fabricating the composite coatings containing HA and other additives. In this way, while maintaining the biocompatibility due to the presence of HA in the composition, other properties, such as adhesion and wear resistance, can be improved [9−14]. In this regard, in addition to composite coatings, another interesting research area is development and production of functionally graded bioactive coatings containing HA. In most non-graded coatings, if there is a difference between the coating material and the substrate, abrupt changes in the properties of the coating, such as elastic modulus, density, Poisson's ratio, and expansion coefficient, increase the residual stress at the interface and deteriorate its physical and mechanical properties. But in the functionally graded coatings, the chemical composition gradually changes and the problem of abrupt change in properties at the interface is solved to a large extent [15−18]. This can be also seen in a natural bone whose cross-section shows a gradual change from a dense hard structure on the outside to a soft porous one in the inside [15].

Different methods have been commonly used to deposit HA-containing coatings on the metallic alloy implants, such as plasma spray [11,14], thermal spray [18,19], electrophoretic deposition [9,20], sol−gel [21], and laser cladding [22]. In some studies, HA/TiO_2 functionally graded coatings (FGCs) were deposited on the Ti−6Al−4V substrates using an electrophoretic deposition method and the coatings with better adhesion and fracture toughness were achieved [23−25]. Moreover, multi-layer bio-glass/HA FGC was deposited on the 316L stainless steel via a plasma spray method and desirable structural and mechanical properties as well as great biocompatibility were obtained [26]. However, almost all the aforementioned processes or at least one of their steps are performed at high temperatures, which can eventually change the crystalline phase or grain size of both the coating and the substrate. High temperature also increases the residual stresses, thereby reducing the adhesion between the coating and the substrate [27].

To overcome the aforementioned problems, mechanical coating techniques (MCTs) have been recently developed and used for deposition of various materials on metal substrates at room temperature [28], where the balls, the coating material (in the form of powders), and the substrate are placed in a vibrating chamber. The powder particles are compressed between the balls and the substrate due to the rapid and continuous impacts of the balls on the substrate, and as a result, the metal surface is coated with the powders. Different metal, ceramic, intermetallic, and composite coatings have been acceptably deposited on different metallic substrates by MCTs. The most important advantage of the coatings deposited by MCTs is that a strong bond can be generated between the coating and the substrate at ambient conditions using a low-cost process [29−33]. However, a limited number of researchers have tried MCTs to deposit HA on implant alloys. In one study, a ball impact process was used to deposit HA coatings on a pure Ti substrate and the parameters (ball diameter, time, and ball filling fraction) were optimized [34]. In another study, the same method was employed for the deposition of an HA/Ti powder mixture on a Ti substrate and denser coatings with better adhesion were produced compared to HA coatings [35]. In this process, the passive oxide film formed on the surface of the Ti substrate is easily fractured and separated under the ball impact, and a suitable strong mechanical bond is created because of interlocking between the powder particles and the surface of the substrate [34−37].

Although a few attempts have been made to produce graded coatings by a mechanical coating process, no research has been reported so far concerning its application to produce a functionally graded composite coating containing HA. For instance, a graded W/Cu composite coating was well-deposited on the Cu substrate by mechanical alloying and a significant improvement in hardness and wear resistance was reported [38]. A Ni−Al_2O_3 FGC was also mechanically plated on an Al substrate by a ball milling process and superior wear properties were achieved compared to the non-graded coatings [39]. To produce a graded composite coating with an MCT process, initially a

layer with a composition close to the metallic substrate is deposited, and then the percent of coating material is augmented in the following layer(s). In this manner, the concentration gradient between the coating and the substrate is reduced. As a result, a coating with better mechanical properties than a non-graded coating is obtained and no sudden changes in the properties occur. Therefore, this research seeks to study the potential of the MCT for depositing graded and non-graded HA/Ti composite coatings on the Ti−6Al−4V alloy substrate and compare their structure, wear resistance, and biocompatibility.

2 Experimental

2.1 Materials

Circular sheets of commercial Ti−6Al−4V alloy (Loterios, Italy) with a diameter of 20 mm and a thickness of 2 mm were used as the substrate material. Their surfaces were ground with 200#, 400#, 600#, and 800# sandpapers and then cleaned with ethanol and distilled water before the coating treatment. HA (Apatech, Iran) and titanium powders (Umicore, Belgium) with particle size of 10−50 μm and purity of 99.5%, were used as the coating materials.

2.2 Deposition setup

A schematic of the mechanical coating process used in this study is shown in Fig. 1. As shown, the desired powders and several balls are placed inside a chamber. By applying vibration, a coating film is formed by a cold welding mechanism as a result of repeated pressures and impacts exerted by the balls. Inspired by the previous researches [31−34], the apparatus was built. One of the advantages of this method is that the desired combination of the coating materials can be achieved. This is a crucial factor for deposition of composite coatings on metallic substrates. In this study, a wear-resistant Teflon chamber with the volume of 50 mm^3 and balls made of bearing steel were used. In order to avoid iron contamination, the mixture of the balls and the desired powders was vibrated for 30 min before the coating treatment.

To fabricate the composite coating, a mixture of 50 wt.% HA and 50 wt.% Ti powder was used. The FGC was produced in two deposition steps. For the first layer, a powder mixture of 75 wt.% Ti and 25 wt.% HA was sued. For the second layer, a mixture of 25 wt.% Ti and 75 wt.% HA was deposited. To determine the process parameters, the results of the previous similar studies were used. The effect of different parameters of the mechanical plating process on the properties of coatings was studied and almost the same results have been obtained. It has been reported that, with increasing the ball-to-powder mass ratio (BPR), time, and ball size, the coating thickness initially increases and then decreases after reaching a maximum value [34,40]. In this study, considering those results, some initial experiments were carried out and then the optimized coating parameters were determined (see Table 1).

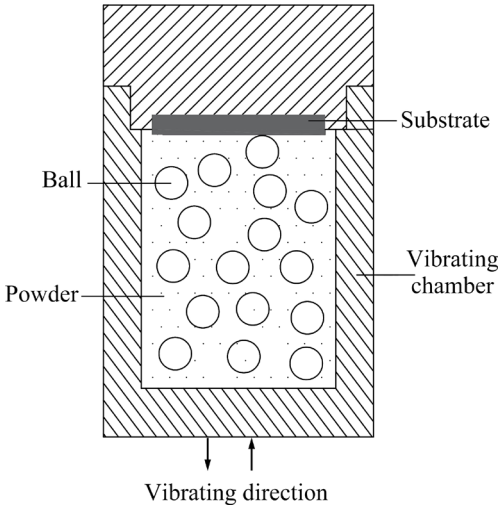

Fig. 1 Schematic of mechanical coating technique (MCT)

Table 1 Optimized coating parameters employed for MCT used in this study

Time duration/ min	Ball diameter/ mm	BPR	Frequency/ Hz	Amplitude/ mm
90	7	7:1	20	30

2.3 Surface characterization

X-ray diffraction (XRD) analysis was carried out using a Philips X'PERT MPD apparatus with the Cu K_α (λ=1.5405 Å) to investigate the presence of different phases in the coatings and identify the changes in the primary powder particles. A voltage of 40 kV, a current of 30 mA, and a step length of 0.02° were employed. Microstructural studies were performed on the deposited surfaces and cross-sections of the coatings using an MIRA3 TESCAN

field emission scanning electron microscope (FE-SEM) equipped with an energy dispersive spectroscopy (EDS) detector. To study the cross-sections, wire cutter was used to cut the specimens. The surface morphology was observed with a scanning probe microscope (Nanowizard 2, JPK, Germany) using atomic force microscopy (AFM). Moreover, elemental analysis of the coatings was performed to study their composition.

2.4 Biocompatibility evaluation

The biological features of the coated surfaces were studied in vitro. For this purpose, the specimens were first placed in 70% ethanol for 30 min, washed in PBS and then both sides of them were sterilized under UV light for 15 min. The viability of the cultured cells was studied via MTT assay. The MC3T3-E1 mouse osteoblast-like cells were cultured in a humidified medium of 5% CO_2 at 37 °C for 24 h. Then, they were seeded on the coated specimens in a 24-well plate at a 10^5 cells/well density, and after 1, 2, 3, and 7 d the culture media were removed. Then, a medium containing 10% MTT (tetrazolium salt) was added to each well and the cells were allowed to be in the vicinity of this new medium at 37 °C for 4 h. Living cells absorb MTT and convert it into insoluble formazan crystals. After that, the culture medium was removed and 50 μL DMSO was added to it to dissolve the formazan crystals. The assessment of cell viability was done by calculating the colored output absorbance by spectrophotometry at 570 nm. All the experiments were done for all four time-points and repeated 3 times. A similar process was performed for MC3T3-E1 cells cultured on culture well surface as the control sample.

To evaluate the morphology and attachment of the cells on the surfaces, after 7 d, the cultured media were removed and the specimens were fixed with 2.5% glutaraldehyde in PBS at room temperature for 1 h. After dehydration in serial diluted ethanol, SEM examinations of the morphology of cultured cells were done.

2.5 Tribology and adhesion strength testing

The wear resistance of the coated samples was evaluated by a pin-on-disk wear test with the applied force of 5 N, the sliding speed of 0.08 m/s, and the total sliding distance of 200 m. The pin was AISI 52100 steel with a hardness of HRC 56 and an electronic balance with an accuracy of 0.1 mg was used for measuring the mass of samples. Their wear behavior was investigated by plotting and comparing the friction coefficient versus the distance travelled by the pin. The mass loss of the samples after the wear test was also measured. The surface roughness (R_a) of the samples after wear test was measured by a TR200 roughness measuring device (Time Group Inc.).

The adhesion strength between the coatings and substrate was measured using a pull-off bonding test machine (PosiTest AT, Defelsko). The testing studs (20 mm in diameter) were glued to the surface of the coated specimens with a two-component epoxy based adhesive and then curing was done at ambient temperature for 24 h. The pull-off test was done at a tensile rate of 1 MPa/s until failure. The reported values are the average of three measurements.

3 Results and discussion

3.1 Phase analysis

Figure 2(a) shows the XRD patterns of the HA/Ti composite coating and FGC. For comparison, the XRD pattern of the initial HA powder is also presented. The peaks with extremely high and low intensities are related to Ti and HA, respectively. As the HA peaks (2θ=26°−36°) in Fig. 2(a) are very small, for a better analysis, they are shown with a higher magnification in Fig. 2(b). As the process was carried out at room temperature, no phase changes or decomposition occurred in the primary powder particles, which is one of its main advantages. Therefore, the HA with its original crystalline structure participates in the coating and can provide appropriate biocompatibility.

Compared with the HA powder feedstock, the XRD patterns show a reduction in the intensity of the HA peaks in both coatings. This might be because the mechanical deformation of the particles during the MCT refines the particles, reduces the crystal size, and increases the micro-strains in the lattice, leading to smaller diffraction areas and broader peaks [41]. A greater reduction in the intensity of HA peaks is also seen in the non-graded HA/Ti composite coating compared to FGCs. This can be attributed to the higher proportion of HA in the top layer of the graded HA/Ti coating.

3.2 Microstructural observation

The macroscopic images of the coatings in comparison with the non-coated Ti−6Al−4V substrate are shown in Fig. 3(a). As seen, the surface of the composite coating is a little darker due to the higher content of Ti, but an acceptable level of coverage is achieved in both composite coating and FGC. Figures 3(b, c) show the SEM images of the coating surfaces. ZADOROZHNYY et al [35] used a mixture of HA and Ti powders with different mass ratios (1:1, 2:1 and 1:2) for their coatings and reported good coverage with the ratio of 1:1 on the pure Ti substrate. Considering the initial particle size of the powders (10−50 μm), Fig. 3 indicates that the particles are fractured into smaller sizes of even less than 5 μm during the coating process. This is due to the fact that the powder particles are compressed between the balls, the balls and the chamber wall, or the balls and the substrate. The morphology and the moderate

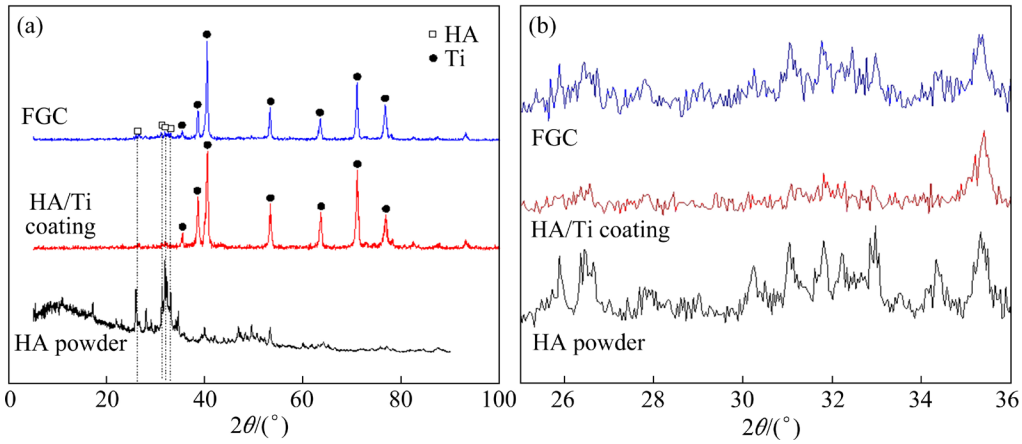

Fig. 2 XRD patterns of HA powder, HA/Ti composite coating and FGC (a), and HA peaks with higher magnification (b)

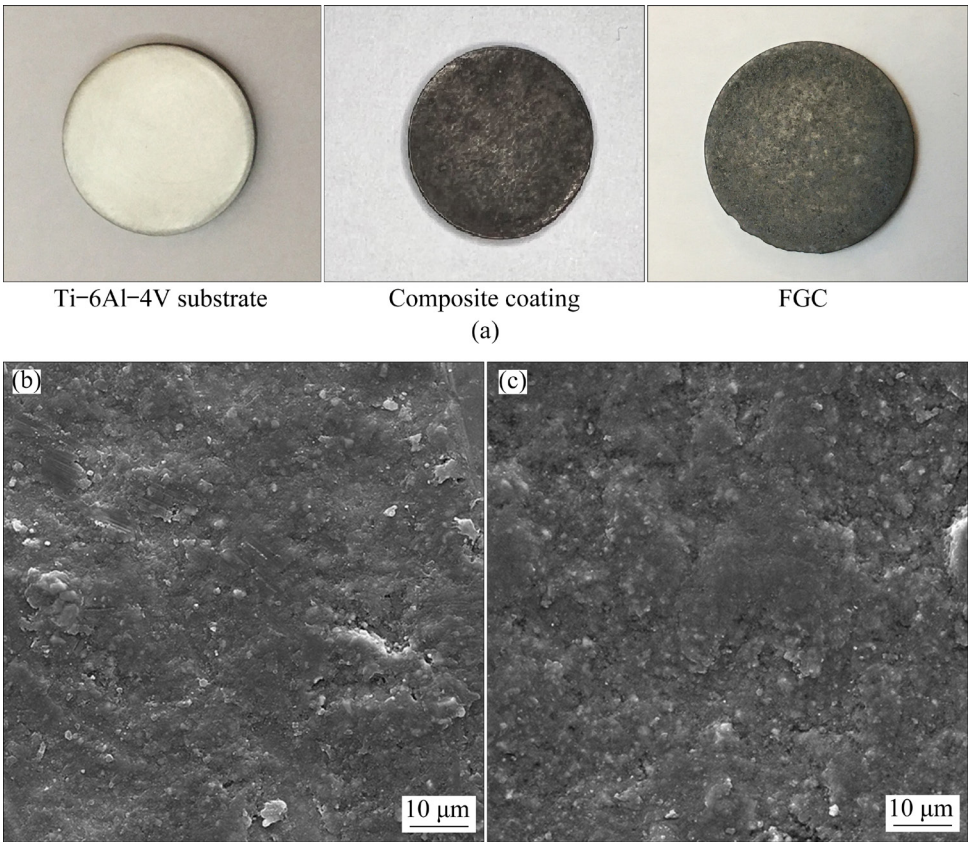

Fig. 3 Macroscopic images of samples with and without coating (a), and SEM images of HA/Ti composite coating (b) and HA/Ti FGC surface (c)

uneven distribution of the coating can be attributed to the mechanism of permanent cold-weld as well as fracture of the particles under the impacts during the deposition process.

Figure 4 illustrates the surface morphology of the coatings obtained by atomic force microscope (AFM). Both of the coatings include up and down hills, but their roughness is significantly different. The peak-to-valley roughness of the composite coating and FGC are about 700 and 250 nm, respectively. However, the AFM images indicate that the FGC (Fig. 4(b)) is constituted of smaller particles compared to the composite coating (Fig. 4(a)), which leads to more contact surface in it. This topography could result more biocompatibility of FGC.

Based on the SEM images of the coating cross-section (Fig. 5), the average thickness of both coatings is 8−10 μm and does not significantly change on the surface. An ideal continuous interface is observed between the coatings and the substrate. This is because the Ti particles in the powder mixture provide the opportunities for mechanical mixing, inter-locking, and consolidating the coating on the substrate. However, due to the presence of 50 wt.% HA in the HA/Ti composite coating (Fig. 5(a)), weaker bonds are observed in some points of the coating/substrate interface.

Figure 5(b) shows the cross-section of the HA/Ti FGC that has two layers. In this figure, the white points are Ti particles whose sizes vary from less than 1 to about 5 μm. After 45 min deposition of the first layer (75 wt.% Ti + 25 wt.% HA) that is in direct contact with substrate, the second layer was deposited with a powder mixture of 25 wt.% Ti + 75 wt.% HA. The composition of the powder mixture used for the second layer was adjusted by adding some HA powders into the deposition chamber and taking out some of the first-layer coating material. Furthermore, the cross-section of graded coating indicates that the first and second layers that contain different amounts of Ti, are so integrated that their interface cannot be easily identified without considering the content gradients of Ti particles between the two layers. YAZDANI and ISFAHANI [39] deposited the graded Ni−Al_2O_3 composite coatings on the aluminum substrate by the MCT and reported the formation of such an interface. This continuous interface can be considered as one of the characteristics of the FGCs produced by the MCT. Nevertheless, in some other FGC deposition methods (e.g. plasma spray,

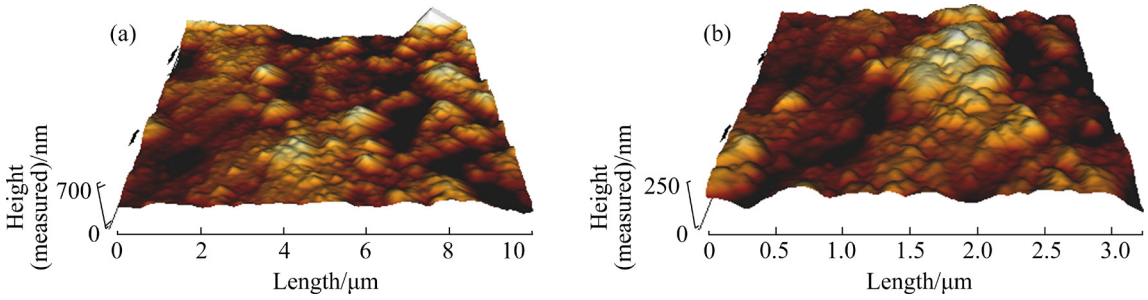

Fig. 4 AFM images of surfaces of composite coating (a) and FGC (b)

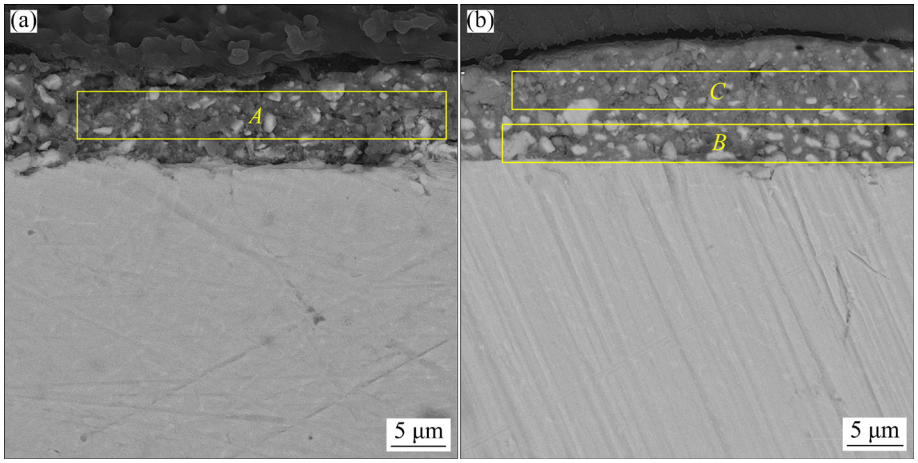

Fig. 5 SEM images of cross-section of HA/Ti composite coating (a) and FGC (b)

electrophoretic, and sputtering), the boundaries between different layers of the coating can be easily observed [23,25,42,43].

In the SEM images of the cross-section of the coatings (Fig. 5), some pores and weak points are seen. Considering that the specimens were cut with wire cutter and due to the inherent brittleness of HA, it is inevitable to create some damages and cracks in the coating during the operation. Furthermore, some of these defects may have been created while preparing specimens for cross-sectional structural study. These pores and cracks in the FGC are significantly less than those in the non-graded composite coating (notably at the coating/substrate interface). On the other hand, most of these defects are limited, discontinuous and small in size (even less than 1 μm).

At the beginning of the MCT deposition, the Ti and HA powders are simultaneously bonded and fractured due to the impacts exerted by the balls, and as the process is repeated, the particles are downsized. Smaller particles can be clearly seen in the cross-sections of both coatings (Fig. 5). Moreover, the powder particles penetrate into the surface of the substrate and better bonding is obtained between the Ti powder and Ti−6Al−4V substrate. In this way, during the coating deposition, a rough and irregular base with appropriate regions is repeatedly generated, thereby more Ti and HA particles can attach to it.

Elemental analysis was performed to determine the approximate chemical composition of the coatings and particularly show the difference in chemical composition between the two layers of FGC (Fig. 6 and Table 2). The EDS analysis of the composite coating obtained from 50 wt.% Ti and 50 wt.% HA powder mixture (Fig. 6(a)) indicates the presence of 25.37 wt.%, 29.39 wt.% and 16.17 wt.% of Ti, Ca and P, respectively. In addition, the EDS analysis of the first and second layers of the FGC, which obtained from powder mixtures containing 75 wt.% and 25 wt.% Ti, respectively, reveals the presence of 55.14 wt.% and 12.8 wt.% Ti. In this coating, the change of the mass fraction of Ca and P from 20.68 wt.% and 8.00 wt.% in the inner layer (Area *B* in Fig. 5(b)) to 32.73 wt.% and 19.69 wt.% in the outer layer (Area *C* in Fig. 5(b)) is clearly evident.

Figure 7 shows the SEM image and corresponding EDS maps of the FGC cross-section.

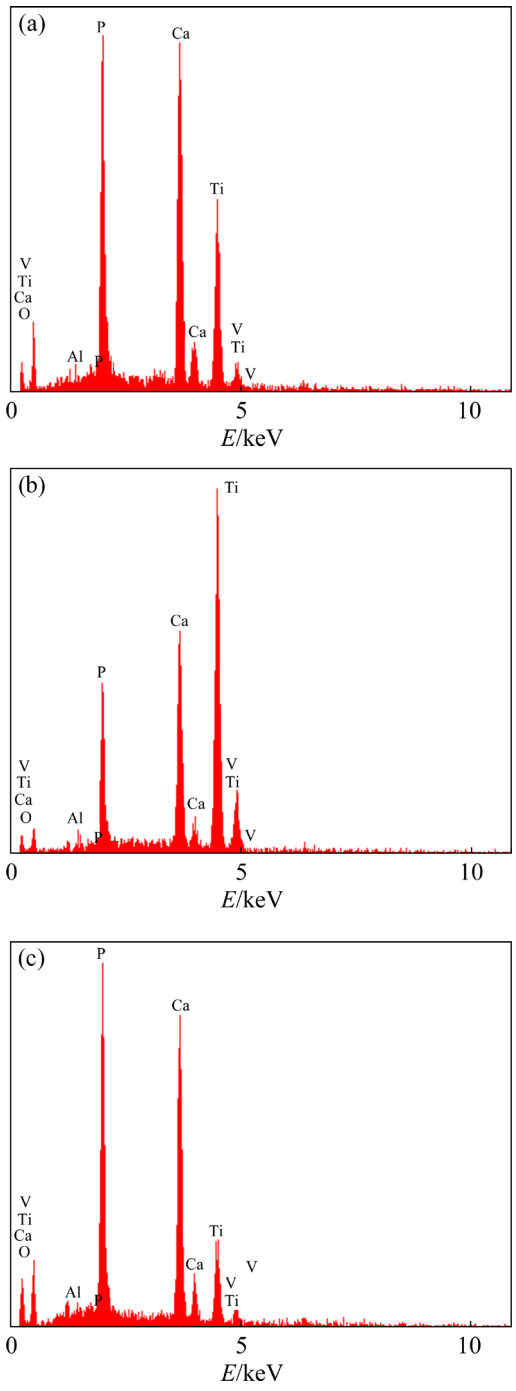

Fig. 6 EDS analysis results of cross-sections of HA/Ti composite: (a) Area *A* in Fig. 5(a); (b) Area *B* in Fig. 5(b); (c) Area *C* in Fig. 5(b)

Table 2 EDS analysis results of Areas *A*, *B*, and *C* in Fig. 5 (wt.%)

Area	O	P	Ca	Ti
A	28.98	16.17	29.39	25.37
B	16.03	8.00	20.68	55.14
C	34.66	19.69	32.73	12.80

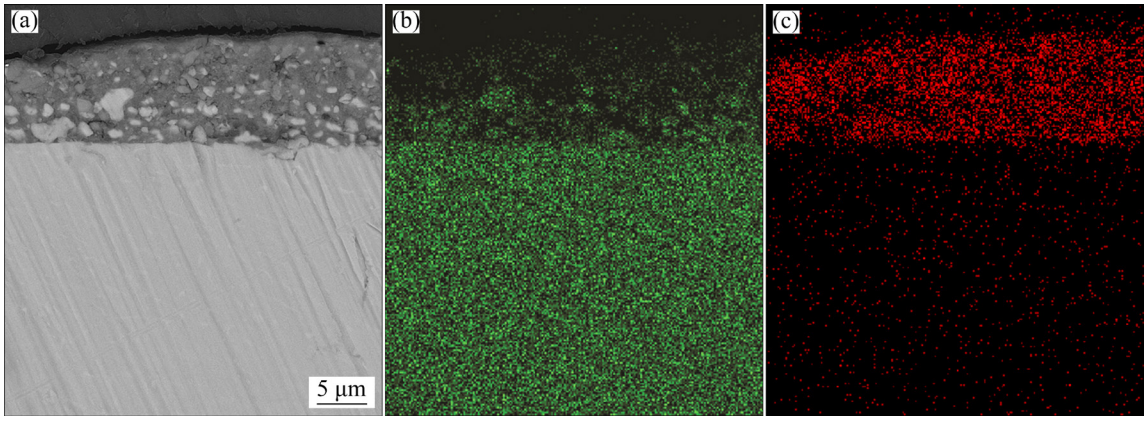

Fig. 7 SEM image (a) and corresponding EDS maps of Ti (b) and Ca (c) in FGC

This analysis was carried out to investigate the distribution of the elements in the coating and identify its graded nature. An almost uniform distribution of Ca (as an indication of the presence of HA) can be seen. However, the Ti distribution is less uniform due to the fragmentation of the primary Ti powder particles. As a result, smaller Ti particles are produced during the deposition process. Therefore, small and large Ti particles are present in the coating at the same time. This leads to a better adhesion between the particles and the substrate and also more contact area with the HA particles during coating formation. Furthermore, the inter-locking between the Ti particles and the substrate at the interface is clearly seen. It should be noted that the primary purpose of using the Ti powder in the coating material was to achieve such an interface.

3.3 Wear behavior and adhesion strength

The results of the wear tests are summarized in Table 3. The coefficient of friction (COF) as a function of sliding distance for composite coating and FGC are presented in Fig. 8. The sliding distance of the coating from the surface to the substrate is 70 m in the HA/Ti composite coating (Fig. 8(a)). The COF and mass loss of the HA/Ti composite coating are 0.37 and 0.0097 g, respectively. As can be seen, the COF is initially around 0.45 and then decreases to a constant value of 0.37 after the sliding distance of about 15 m. The high COF in the early stages of the wear test can be attributed to the higher roughness and the greater amount of Ti present on the surface of this coating. In the case of FGC (Fig. 8(b)), the graph shows a gradual increase in the COF. This is mainly because the amount of Ti increases gradationally while moving from the surface to the interface, representing and confirming the graded nature of the FGC. In addition, the gradual change of the COF in FGC indicates its better adhesion to the substrate. For the

Table 3 Wear test results of coatings

Coating	R_a/μm	COF	Mass loss/g
HA/Ti composite	2.712	0.37	0.0097
FGC	1.465	0.32−0.5	0.0098

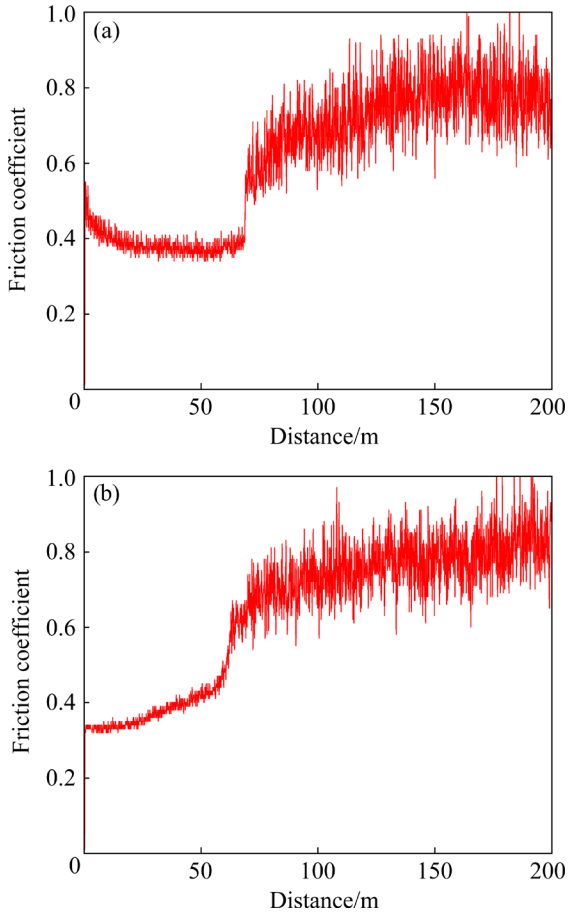

Fig. 8 Friction coefficient of coatings versus sliding distance: (a) HA/Ti composite coating; (b) FGC

FGC, the worn distance from the coating surface to the substrate is about 65 m. The initial COF is 0.32, which is related to the surface, and reaches 0.5 at the interface. Its mass loss is 0.0098 g. Figures 8(a, b) also indicate the better and more uniformed frictional behavior of the coatings compared with the substrate. Therefore, the COF is lower with very limited fluctuations until the sliding distances of 65 and 70 m where the coatings are under wear. However, as the wear of the substrate starts, the COF and fluctuations significantly increase due to the poor tribological properties of the Ti alloy substrate.

There have been no reports so far on the wear test of HA/Ti coatings deposited on the substrates of medical implant alloys by the MCT and most studies have investigated the coatings obtained by other methods. However, ZADOROZHNYY et al [35] studied the tribological behavior of mechanically-deposited HA/Ti coatings on the pure Ti substrate via a scratch test and obtained the COF of 0.33−0.5, which is close to the values obtained in the present work (Fig. 8). To improve the microstructure, crystallinity and wear properties of HA-containing coatings deposited on the implant alloys by thermal processes, post heat treatment is usually carried out [11,27,43−45]. KUMARI and MAJUMDAR [45] also studied the wear properties of HA/TiO_2 composite coatings on the Ti−6Al−4V substrate before and after the heat treatment. Their results showed COF of 0.7−0.87 for the uncoated substrate and COF of 0.8−0.9 for the non-heat-treated coating. But after the heat treatment, the COF fell within the range of 0.6−0.7 and the wear behavior was improved due to the lower roughness and porosity of the surface and higher hardness caused by the heat treatment. However, the COF of the MCT-deposited HA/Ti coatings in this study is within a more appropriate range (0.32−0.5).

The SEM images of the worn surfaces (Fig. 9) show the dominance of abrasive wear mechanism for both coatings. In fact, higher hardness and brittleness of the HA particles lead to more fragmentation during the deposition process, and as a result, finer particles are produced. Therefore, during the wear test, the HA particles detached from the coating generate finer scratches on the surface. The effect of adhesive wear is also seen on the worn surface of the HA/Ti composite coating (Fig. 9(a)), which can be due to the squashing of the abrasive pin on the substrate.

The adhesion strengths of composite coating and FGC to the substrate are 13 and 21 MPa, respectively. The significant superior bonding strength of FGC could be attributed to the more connection points at the coating/substrate interface, which is due to the higher content of Ti particles. The adhesion strength of FGC which is the average of 3 specimens is (21±3) MPa (ranging between 18 and 24 MPa) that is higher than the ISO 13779—2 requirement (15 MPa). In addition, the gradual change of the COF in FGC compared to composite coating (Fig. 7) indicates its better adhesion to the substrate.

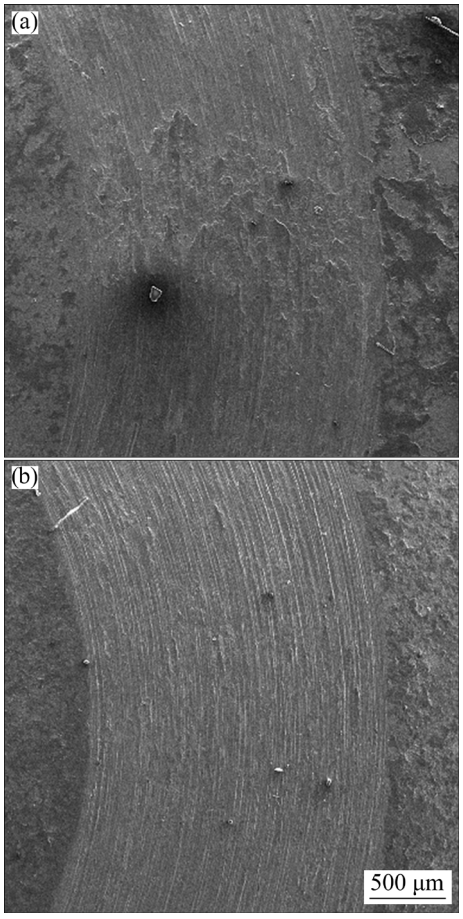

Fig. 9 SEM images of worn surfaces of HA/Ti composite coating (a) and FGC (b)

3.4 In vitro biological evaluation

3.4.1 Cell attachment

The attachment of cells to the surface of biomaterials is one of the important biological properties indicating their biocompatibility. The SEM images of the morphology of MC3T3-E1 cells attached on the Ti−6Al−4V substrate and coatings are shown in Fig. 10. The results indicate weak cell

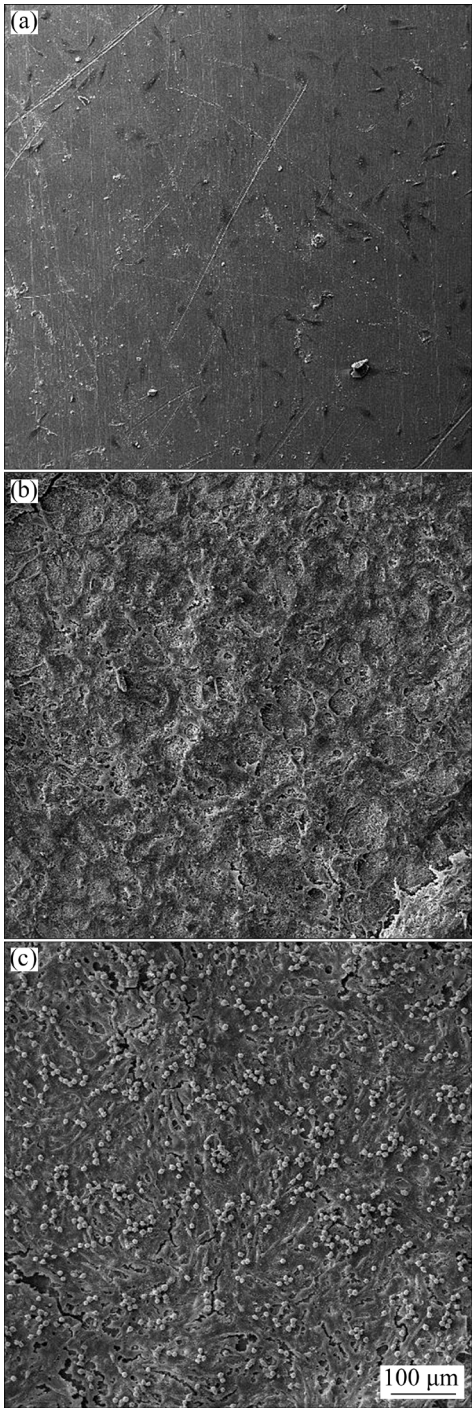

Fig. 10 SEM images of MC3T3-E1 cells attached on surface of Ti−6Al−4V substrate (a), 50 wt.% HA + 50 wt.% Ti composite coating (b), and FGC (c) after 7 d

attachment on the substrate surface (Fig. 10(a)) and good cell attachment and morphology in both coatings (Figs. 10(b, c)). As can be seen, in the coated specimens the cells cover almost the entire surface and are attached and completely spread on the surface. However, Fig. 10(c) shows better cell attachment on the surface coated by FGC in comparison with that coated by 50 wt.% HA + 50 wt.% Ti composite (Fig. 10(b)). This can be attributed to the presence of higher amounts of HA on the surface of the FGC.

3.4.2 Statistical analysis of cell viability

A cytotoxic effect is defined as a reduction of more than 30% in cell viability according to the ISO 10993—5 standard for in vitro cytotoxicity assessment of medical devices. MTT assay was performed to assess the cytotoxicity of coated specimens. Figure 11 compares the cell viability after 1, 2, 3, and 7 d of culture on the control and coated specimens. Each cell viability is the average of tests on three specimens and was calculated by comparing it to the control. The cell viability of control was considered 100%. The results indicate an increase in the cell viability and proliferation on the surface of the coated specimens. The viability of MC3T3-E1 cells after 7 d was increased from (76±7.1)% in the uncoated Ti−6Al−4V sample to (83±4.2)% and (85±3.0)% in the composite coating and FGC, respectively. Moreover, this figure shows that the coated surfaces have good biocompatibility with viability over 80% of control at all culturing time and also the cell viability is not significantly different between the two coated specimens.

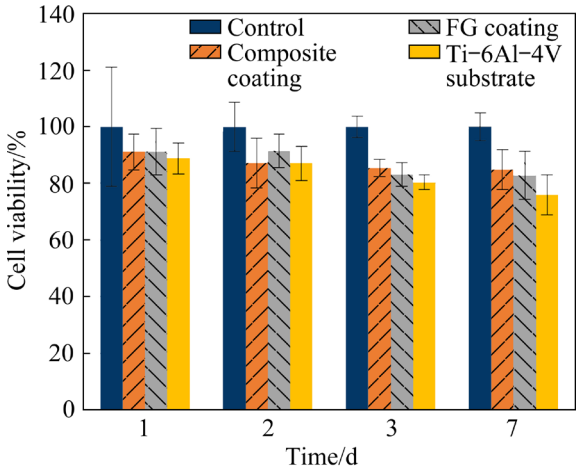

Fig. 11 Statistical evaluation of viability of MC3T3-E1 cells after 1, 2, 3, and 7 d of culture on composite coating, FGC, and uncoated surfaces using MTT assay

4 Conclusions

(1) The XRD results showed no phase changes in the powder particles used for the coatings production because the deposition process was carried out at ambient temperature.

(2) Ti particles helped to form an integrated

interface between the coatings and the substrate, especially in the FGC, due to the higher ratio of Ti in contact with the substrate. A perfect continuous interface between the different layers of the FGC, which contained different amounts of Ti, was also observed.

(3) During the wear test of composite coating and FGC, the abrasive pin came into contact with the surface of the substrates after sliding distance of 70 and 65 m, respectively. For the composite coating, the COF was almost constant (0.37) with a sharp increase at the interface. But for the FGC, the COF gradually increased from 0.32 to 0.5 by moving from the surface of the coating to the interface with a steadily increase at the interface. Abrasive wear was the dominant mechanism and mass loss was approximately the same for both coatings.

(4) The in vitro biological evaluation showed the suitable cell viability of both coatings and better cell attachment and proliferation of the FGC.

CRediT authorship contribution statement

Mahmood JALALI BIDAKHAVIDI: Investigation, Methodology, Writing origin-draft, Writing − Review & editing, Funding acquisition; **Hamid OMIDVAR:** Investigation, Conceptualization, Supervision, Writing − Review & editing; **Ali ZAMANIAN:** Investigation, Conceptualization, Supervision, Data curation; **Jamshid AGHAZADEH MOHANDESI:** Conceptualization, Supervision; **Hamid JALALI:** Data curation, Resources.

Declaration of competing interest

The authors declare that they have no known competing financial interests or personal relationships that could have appeared to influence the work reported in this paper.

References

[1] KATTI K S. Biomaterials in total joint replacement [J]. Colloids and Surfaces B: Biointerfaces, 2004, 39: 133−142.

[2] CHEN Q Z, THOUAS G A. Metallic implant biomaterials [J]. Materials Science and Engineering: R, 2015, 87: 1−57.

[3] KRELLER T, SAHM F, BADER R, BOCCACCINI A R, JONITZ-HEINCKE A, DETSCH R. Biomimetic calcium phosphate coatings for bioactivation of titanium implant surfaces: Methodological approach and in vitro evaluation of biocompatibility [J]. Materials, 2021, 14: 3516.

[4] ZAKARIA A, SHUKOR H, TODOH M, JUSOFF K. Bio-functional coating on Ti6Al4V surface produced by using plasma electrolytic oxidation [J]. Metals, 2020, 10: 1124.

[5] HEIMANN R B. The challenge and promise of low-temperature bioceramic coatings: An editorial [J]. Surface and Coatings Technology, 2016, 301: 1−5.

[6] WEI Q, CUI Z D, YANG X J, ZHANG L Y, DENG J Y. Design and characterization of bioceramic coating materials for Ti6Al4V [J]. Frontiers of Materials Science in China, 2010, 4: 171−174.

[7] MCENTIRE B, BAL B S, RAHAMAN M N, CHEVALIER J, PEZZOTTI G. Ceramics and ceramic coatings in orthopaedics [J]. Journal of the European Ceramic Society, 2015, 35: 4327−4369.

[8] DOROZHKIN S V. Calcium orthophosphate bioceramics [J]. Ceramics International, 2015, 41: 13913−13966.

[9] RATH P C, BESRA L, SINGH B P, BHATTACHARJEE S. Titania/hydroxyapatite bi-layer coating on Ti metal by electrophoretic deposition: Characterization and corrosion studies [J]. Ceramics International, 2012, 38: 3209−3216.

[10] BALANI K, CHEN Y, HARIMKAR S P, DAHOTRE N B, AGARWAL A. Tribological behavior of plasma-sprayed carbon nanotube-reinforced hydroxyapatite coating in physiological solution [J]. Acta Biomaterialia, 2007, 3: 944−951.

[11] KUMARI R, MAJUMDAR J D. Microstructure and surface mechanical properties of plasma spray deposited and post spray heat treated hydroxyapatite (HA) based composite coating on titanium alloy (Ti−6Al−4V) substrate [J]. Materials Characterization, 2017, 131: 12−20.

[12] LIN M H, CHEN Y C, LIAO C C, LIN L W, CHEN C F, WANG K K, CHEN S T, HSUEH Y H, WU C H, OU S F. Improvement in bioactivity and corrosion resistance of Ti by hydroxyapatite deposition using ultrasonic mechanical coating and armoring [J]. Ceramics International, 2022, 48: 4999−5008.

[13] SINGH J, CHATHA S S, SINGH H. Characterization and corrosion behavior of plasma sprayed calcium silicate reinforced hydroxyapatite composite coatings for medical implant applications [J]. Ceramics International, 2021, 47: 782−792.

[14] SINGH H, KUMAR R, PRAKASH C, SINGH S. HA-based coating by plasma spray techniques on titanium alloy for orthopedic applications [J]. Materials Today: Proceedings, 2022, 50: 612−628.

[15] ROY S. Functionally graded coatings on biomaterials: A critical review [J]. Materials Today Chemistry, 2020, 18: 100375.

[16] FATHI R, WEI H, SALEH B, RADHIKA N, JIANG J H, MA A B, AHMED M H, LI Q, OSTRIKOV K K. Past and present of functionally graded coatings: Advancements and future challenges [J]. Applied Materials Today, 2022, 26: 101373.

[17] SATHISH M, RADHIKA N, SALEH B. A critical review on functionally graded coatings: Methods, properties, and challenges [J]. Composites Part B: Engineering, 2021, 225: 109278.

[18] ŁATKA L, PAWŁOWSKI L, WINNICKI M, SOKOŁOWSKI P, MAŁACHOWSKA A, KOZERSKI S.

Review of functionally graded thermal sprayed coatings [J]. Applied Sciences, 2020, 10: 5153.

[19] KULPETCHDARA K, LIMPICHAIPANIT A, RUJIJANAGUL G, RANDORN C, CHOKETHAWAI K. Influence of the nano hydroxyapatite powder on thermally sprayed HA coatings onto stainless steel [J]. Surface and Coatings Technology, 2016, 306: 181−186.

[20] KWOK C T, WONG P K, CHENG F T, MAN H C. Characterization and corrosion behavior of hydroxyapatite coatings on Ti6Al4V fabricated by electrophoretic deposition [J]. Applied Surface Science, 2009, 255: 6736−6744.

[21] ROEST R, LATELLA B A, HENESS G, BEN-NISSAN B. Adhesion of sol–gel derived hydroxyapatite nanocoatings on anodised pure titanium and titanium (Ti6Al4V) alloy substrates [J]. Surface and Coatings Technology, 2011, 205: 3520−3529.

[22] JING Z, CAO Q Q, JUN H. Corrosion, wear and biocompatibility of hydroxyapatite bio-functionally graded coating on titanium alloy surface prepared by laser cladding [J]. Ceramics International, 2021, 47: 24641−24651.

[23] ARAGHI A, HADIANFARD M J. Fabrication and characterization of functionally graded hydroxyapatite/TiO_2 multilayer coating on Ti–6Al–4V titanium alloy for biomedical applications [J]. Ceramics International, 2015, 41: 12668−12679.

[24] FARNOUSH H, MOHANDESI J A, ÇIMENOĞLU H. Micro-scratch and corrosion behavior of functionally graded HA-TiO_2 nanostructured composite coatings fabricated by electrophoretic deposition [J]. Journal of the Mechanical Behavior of Biomedical Materials, 2015, 46: 31−40.

[25] FARNOUSH H, ALDıÇ G, ÇIMENOĞLU H. Functionally graded HA–TiO_2 nanostructured composite coating on Ti−6Al−4V substrate via electrophoretic deposition [J]. Surface and Coatings Technology, 2015, 265: 7−15.

[26] CATTINI A, BELLUCCI D, SOLA A, PAWŁOWSKI L, CANNILLO V. Suspension plasma spraying of optimised functionally graded coatings of bioactive glass/ hydroxyapatite [J]. Surface and Coatings Technology, 2013, 236: 118−126.

[27] BARRY J N, TWOMEY B, COWLEY A, O'NEILL L, MCNALLY P J, DOWLING D P. Evaluation and comparison of hydroxyapatite coatings deposited using both thermal and non-thermal techniques [J]. Surface and Coatings Technology , 2013, 226: 82−91.

[28] SAVRAI R A, MOROZOVA A N. A review of studies in the field of production of coatings on metals by means of mechanical alloying [J]. Surfaces and Interfaces, 2021, 27: 101451.

[29] ROMANKOV S, HAYASAKA Y, KASAI E, YOON J M. Fabrication of nanostructured Mo coatings on Al and Ti substrates by ball impact cladding [J]. Surface and Coatings Technology, 2010, 205: 2313−2321.

[30] HAYASHI N, OKI T. Diamond-like carbon coatings fabricated by the ball impact process [J]. Chemical Engineering Journal, 2014, 237: 455−461.

[31] ROMANKOV S, KOMAROV S V, VDOVICHENKO E, HAYASAKA Y, HAYASHI N, KALOSHKIN S D, KASAI E. Fabrication of TiN coatings using mechanical milling techniques [J]. International Journal of Refractory Metals and Hard Materials, 2009, 27: 492−497.

[32] ZADOROZHNYY V Y, SHAHZAD A, PAVLOV M D, KOZAK D S, CHIRKOV A M, ZAGREBIN D S, KHASENOVA R S, KOMAROV S V, KALOSHKIN S D. Synthesis of the Ni−Al coatings on different metallic substrates by mechanical alloying and subsequent laser treatment [J]. Journal of Alloys and Compounds, 2017, 707: 351−357.

[33] ROMANKOV S, KALOSHKIN S D, HAYASAKA Y, SAGDOLDINA Z, KOMAROV S V, HAYASHI N, KASAI E. Structural evolution of the Ti−Al coatings produced by mechanical alloying technique [J]. Journal of Alloys and Compounds, 2009, 483: 386−388.

[34] HAYASHI N, UENO S, KOMAROV S V, KASAI E, OKI T. Fabrication of hydroxyapatite coatings by the ball impact process [J]. Surf Coat Technol, 2012, 206: 3949−3954.

[35] ZADOROZHNYY V Y, KAEVITSER E V, KOPYLOV A N, BORISOVA Y V, SUDARCHIKOV V V, KHASENOVA R S, GORSHENKOV M V, ZADOROZHNYY M Y, KALOSHKIN S D. Synthesis of the hydroxyapatite coatings on the Ti substrates by mechanical alloying [J]. Surface and Coatings Technology, 2015, 281: 157−163.

[36] KOMAROV S V, ROMANKOV S E, HAYASHI N, KASAI E. Nanostructured coatings produced by a novel ultrasonic-assisted method: Coating characterisation and formation mechanism [J]. Surface and Coatings Technology, 2010, 204: 2215−2222.

[37] ROMANKOV S, HAYASAKA Y, SHCHETININ I V, KASAI E, KOMAROV S V, YOON J M. Investigation of structural formation of Al−SiC surface composite under ball collisions [J]. Materials Science and Engineering: A, 2011, 528: 3455−3462.

[38] MENG Y F, ZHANG J P, DUAN C Y, CHEN C, FENG X M, SHEN Y F. Microstructures and properties of W−Cu functionally graded composite coatings on copper substrate via high-energy mechanical alloying method [J]. Advanced Powder Technology, 2015, 26: 392−400.

[39] YAZDANI A, ISFAHANI T. Hardness, wear resistance and bonding strength of nano structured functionally graded Ni−Al_2O_3 composite coatings fabricated by ball milling method [J]. Advanced Powder Technology, 2018, 29: 1306−1316.

[40] ROMANKOV S, KALOSHKIN S D, HAYASAKA Y, HAYASHI N, KASAI E, KOMAROV S V. Effect of process parameters on the formation of Ti–Al coatings fabricated by mechanical milling [J]. Journal of Alloys and Compounds, 2009, 484: 665−673.

[41] HANNORA A, MAMAEVA A, MANSUROV Z. X-ray investigation of Ti-doped hydroxyapatite coating by mechanical alloying [J]. Surface Review and Letters, 2009, 16: 781−786.

[42] CUI W F, QIN G W, DUAN J Z, WANG H. A graded nano-TiN coating on biomedical Ti alloy: Low friction coefficient, good bonding and biocompatibility [J]. Materials Science and Engineering: C, 2017, 71: 520−528.

[43] CANNILLO V, LUSVARGHI L, SOLA A, BARLETTA M. Post-deposition laser treatment of plasma sprayed titania-hydroxyapatite functionally graded coatings [J]. Journal of the European Ceramic Society, 2009, 29: 3147−3158.

[44] ZHAO G L, WEN G W, WU K. Influence of processing parameters and heat treatment on phase composition and microstructure of plasma sprayed hydroxyapatite coatings [J]. Transactions of Nonferrous Metals Society of China, 2009, 19(Suppl.): 463−469.

[45] KUMARI R, MAJUMDAR J D. Wear behavior of plasma spray deposited and post heat-treated hydroxyapatite (HA)-based composite coating on titanium alloy (Ti−6Al−4V) substrate [J]. Metallurgical and Materials Transactions A, 2018, 49: 3122−3132.

用机械涂层技术在 Ti−6Al−4V 基体表面沉积 HA/Ti 复合涂层与功能梯度涂层的表征、磨损行为和生物相容性

Mahmood JALALI BIDAKHAVIDI[1], Hamid OMIDVAR[1], Ali ZAMANIAN[2], Jamshid AGHAZADEH MOHANDESI[1], Hamid JALALI[3]

1. Department of Materials and Metallurgical Engineering, Amirkabir University of Technology (Tehran Polytechnic), Hafez Ave, P.O. Box 15875-4413, Tehran, Iran;
2. Department of Nanotechnology and Advanced Materials, Materials and Energy Research Center, Karaj, Iran;
3. School of Dentistry, Tehran University of Medical Sciences, Tehran, Iran

摘　要：采用机械涂层技术在 Ti−6Al−4V 基体表面沉积 HA/Ti 复合涂层与功能梯度涂层(FGC)，对涂层进行表征，对比其磨损行为和生物相容性。制备复合涂层所用初始粉末为 50% Ti (质量分数)和 50% HA (质量分数)的混合粉末，而 FGC 分为两层，分别为 75% Ti + 25% HA 和 25% Ti + 75% HA (质量分数)。XRD 结果表明在沉积过程中没有发生相变。此外，由于原始混合粉末中存在 Ti 颗粒，在涂层和基体之间形成了结合良好的连续界面，特别是在功能梯度涂层样品中。磨损实验结果显示，非梯度复合涂层的摩擦因数约为 0.37，在界面处发生突变，而功能梯度涂层的摩擦因数从 0.32 增加到 0.5，在界面处发生平缓变化。磨损表面的 SEM 像表明涂层的主要磨损机制为磨粒磨损。生物相容性评价结果显示，FGC 样品具有更好的细胞黏附和增殖能力。

关键词：机械涂层技术；羟基磷灰石；Ti−6Al−4V 基体；功能梯度涂层；摩擦因数

(Edited by Xiang-qun LI)